Chemical Rescue in Catalysis by Human Carbonic Anhydrases II and III[†]

Haiqian An,[‡] Chingkuang Tu,[‡] David Duda,[§] Ileana Montanez-Clemente,[‡] Kristen Math,[‡] Philip J. Laipis,[§] Robert McKenna,*[,§] and David N. Silverman*[,§]

Department of Pharmacology and Therapeutics and Department of Biochemistry and Molecular Biology, University of Florida College of Medicine, Gainesville, Florida 32610-0267

Received November 19, 2001

ABSTRACT: The maximal velocity of catalysis of CO_2 hydration by human carbonic anhydrase II (HCA II) requires proton transfer from zinc-bound water to solution assisted by His 64. The catalytic activity of a site-specific mutant of HCA II in which His 64 is replaced with Ala (H64A HCA II) can be rescued by exogenous proton donors/acceptors, usually derivatives of imidazole and pyridine. X-ray crystallography has identified Trp 5 as a binding site of the rescue agent 4-methylimidazole (4-MI) on H64A HCA II. This binding site overlaps with the "out" position in which His 64 in wild-type HCA II points away from the zinc. Activation by 4-MI as proton donor/acceptor in catalysis was determined in the dehydration direction using ^{18}O exchange between CO_2 and water and in the hydration direction by stopped-flow spectrophotometry. Replacement of Trp 5 by Ala, Leu, or Phe in H64A HCA II had no significant effect on enhancement by 4-MI of maximal rate constants for proton transfer in catalysis to levels near 10^5 s^{-1}. This high activity for chemical rescue indicates that the binding site of 4-MI at Trp 5 in H64A HCA II appears to be a nonproductive binding site, although it is possible that a similarly effective pathway for proton transfer exists in the mutants lacking Trp 5. Moreover, the data suggest that the out position of His 64 considered alone is not active in proton transfer in HCA II. In contrast to isozyme II, the replacement of Trp 5 by Ala in HCA III abolished chemical rescue of k_{cat} by imidazole but left k_{cat}/K_m for hydration unchanged. This demonstrates that Trp 5 contributes to the predominant productive binding site for imidazole, with a maximal level for the rate constant of proton transfer near 10^4 s^{-1}. This difference in the susceptibility of CA II and III to chemical rescue may be related to the more sterically constrained and electrostatically positive nature of the active site cavity of CA III compared with CA II. The possibility of nonproductive binding sites for exogenous proton donors offers an explanation for the unusually low value of the intrinsic kinetic barrier obtained by application of Marcus theory to chemical rescue of H64A HCA II.

The carbonic anhydrases (CA)[1] catalyze the hydration/dehydration of CO_2/HCO_3^- and appear in three structurally unrelated classes, α, *β*, and *γ*, those in the α class comprising mostly the animal carbonic anhydrases (*1*). The carbonic anhydrases of the well-studied α class have molecular mass near 30 kDa and catalyze the hydration of CO_2 in two separate and distinct stages, the first involving the conversion of CO_2 to HCO_3^- (eq 1) and the second involving the proton transfer steps to regenerate the zinc-bound hydroxide (*2*, *3*).

$$CO_2 + EZnOH^- \rightleftarrows EZnHCO_3^- \overset{+H_2O}{\rightleftharpoons} EZnH_2O + HCO_3^- \quad (1)$$

$$EZnH_2O + B \rightleftarrows EZnOH^- + BH^+ \quad (2)$$

Here B indicates a proton acceptor that may be an exogenous buffer or a residue of the enzyme. There has been considerable literature on the function of His 64 in HCA II as a proton shuttle in the catalysis (*4*−*6*). The proton transfer steps of eq 2 have been determined to be rate-determining under maximal velocity conditions for catalysis by HCA II (*4*) which uses His 64 in proton transfer, whereas HCA III has no prominent donor in catalysis having a Lys at position 64 (*1*). The carbonic anhydrases show enhancement or chemical rescue of the maximal velocity of catalysis upon addition of exogenous proton donors and acceptors that contribute to the proton transfer between the zinc-bound water and solution (*2*−*6*). In this aspect, these exogenous donors/acceptors act as second substrates in the catalysis, showing activation of catalysis that follows Michaelian kinetics. The mutant H64A HCA II provides a form of carbonic anhydrase, like HCA III, in which there is no prominent proton donor in catalysis. Duda et al. (*7*) showed that the proton donor 4-methylimi-

[†] This work was supported by a grant from the National Institutes of Health (GM25154).

* Corresponding authors. D.N.S.: Box 100267, Health Center, University of Florida, Gainesville, FL 32610-0267. E-mail: silvermn@college.med.ufl.edu. Phone: (352) 392-3556. Fax: (352) 392-9696. R.M.: Box 100245, Health Center, University of Florida, Gainesville, FL 32610-0245. E-mail: rmckenna@ufl.edu. Phone: (352) 392-5696. Fax: (352) 392-3422.

[‡] Department of Pharmacology and Therapeutics.

[§] Department of Biochemistry and Molecular Biology.

[1] Abbreviations: HCA III, human carbonic anhydrase III; H64A HCA II, the site-specific mutant of human carbonic anhydrase II in which His 64 has been replaced by Ala; 4-MI, 4-methylimidazole; MALDI-TOF mass spectrometry, matrix-assisted laser desorption/ionization time of flight mass spectrometry; SHIE, solvent hydrogen isotope effect; $R_{H_2O}/[E]$, the proton transfer dependent rate constant for the release of ^{18}O-labeled water from the active site (eq 4); R_1, the rate of catalyzed interconversion of CO_2 and bicarbonate (eq 3).

10.1021/bi0120695 CCC: $22.00
Published on Web 02/08/2002

dazole (4-MI) enhanced catalysis by H64A HCA II at the stage of catalysis involving proton transfer to the zinc-bound hydroxide in the dehydration direction. This effect was also demonstrated in the CO_2 hydration direction using imidazole and 1-methylimidazole (*5*).

Crystallographic structural studies by Duda et al. (*7*) have identified Trp 5 as a binding site of the rescue agent 4-MI on H64A HCA II. Forming a π-stacking interaction with the indole ring of Trp 5, 4-MI at this binding site extends into the active site cavity with the N1 and N3 nitrogens of 4-MI 13.4 and 12.1 Å away from the zinc (*7*). Although hydrogen bonded to solvent molecules in the active site cavity, 4-MI in this binding site forms no hydrogen bonds or strong electrostatic interactions with other residues of the protein. This site in wild-type HCA II overlaps the "out" position in which the side chain of His 64 points away from the zinc (*8*). It is interesting that the imidazole ring of histamine binds at another site in the active site cavity of HCA II, forming an apparent hydrogen bond with Asn 62 and Gln 92 but no prominent interaction with Trp 5 (*9*). The crystal structure of H64A HCA II (*7*) is nearly identical with that of the native enzyme HCA II (*10*); the root-mean-square deviation for Cα atoms is 0.32 Å in comparing these two structures (*7*). Human carbonic anhydrase III has been very difficult to crystallize, and no crystal structure is available. However, we have modeled the structure for HCA III on the basis of the crystal structure of rat CA III (*11*), which has a 90.4% amino acid identity with human CA III used in this study.

We have investigated the effects of 4-MI on site-specific mutants of HCA II and HCA III in which the binding site Trp 5 is replaced with other residues. Activation by 4-MI as proton donor/acceptor in catalysis was determined using ^{18}O exchange between CO_2 and water and stopped-flow spectrophotometry. We have found that the binding site of 4-MI at Trp 5 in H64A HCA II appears to be a nonproductive binding site, although it is possible that a similarly effective pathway for chemical rescue exists in the mutants with replacements of Trp 5. However, in HCA III the binding of imidazole at Trp 5 appears to be a pathway for chemical rescue. The existence of nonproductive binding sites for chemical rescue agents in HCA II provides a possible explanation for extensively curved free energy plots that yield unusually small values of the Marcus intrinsic energy barrier for proton transfer.

MATERIALS AND METHODS

Enzymes. Expression vectors containing the human CA II and CA III coding regions and those of the mutants at positions 5 and 64 were constructed as described by Tanhauser et al. (*12*). All constructs were verified by DNA sequencing of the coding region. The expression plasmids were transformed into *Escherichia coli* BL21(DE3)pLysS (*13*) and gave high-level protein expression (up to 10 mg/L after purification). The identity of the protein products was consistent with molecular masses determined by MALDI-TOF mass spectrometry.

Purification of HCA II variants was performed by affinity chromatography using *p*-(aminomethyl)benzenesulfonamide coupled to agarose beads (*14*). W5A HCA III was purified by gel filtration followed by ion-exchange chromatography (*15*). Electrophoresis on a 10% polyacrylamide gel stained with Coomassie Blue was used to confirm the purity of all enzyme samples which were greater than 95% pure. Concentrations of HCA II and mutants were determined by titration of the active site with the tight-binding inhibitor ethoxzolamide, measuring ^{18}O exchange between CO_2 and water (see below). The concentration of CA III was determined from its molar absorptivity $6.2 \times 10^4\ M^{-1}\ cm^{-1}$ at 280 nm (*16*).

Oxygen-18 Exchange. This method is based on the measurement by membrane-inlet mass spectrometry of the exchange of ^{18}O between CO_2 and water at chemical equilibrium (*17*, *18*) (eqs 3 and 4). An Extrel EXM-200 mass

$$HCOO^{18}O^- + EZnH_2O \rightleftarrows EZnHCOO^{18}O^- \rightleftarrows COO + EZnO^{18}H^- \quad (3)$$

$$EZnO^{18}H^- + BH^+ \rightleftarrows EZnH_2{}^{18}O + B \xrightarrow{+H_2O} EZnH_2O + H_2{}^{18}O + B \quad (4)$$

spectrometer with a membrane-inlet probe (*18*) was used to measure the isotopic content of CO_2. Solutions contained 25 mM total concentration of all species of CO_2 unless otherwise indicated.

This approach yields two rates for the ^{18}O exchange catalyzed by carbonic anhydrase (*18*). The first is R_1, the rate of exchange of CO_2 and HCO_3^- at chemical equilibrium, as shown in eq 5. Here $k_{cat}{}^{ex}$ is a rate constant for maximal

$$R_1/[E] = k_{cat}{}^{ex}[S]/(K_{eff}{}^{S} + [S]) \quad (5)$$

interconversion of substrate and product, $K_{eff}{}^{S}$ is an apparent binding constant for substrate to enzyme, and [S] is the concentration of substrate, either CO_2 or bicarbonate (*19*). The ratio $k_{cat}{}^{ex}/K_{eff}{}^{S}$ is, in theory and in practice, equal to k_{cat}/K_m obtained by steady-state methods. The binding of CO_2 and HCO_3^- to the active site of carbonic anhydrase is weak; for example, the binding constant of CO_2 to CA II is estimated near 100 mM (*19*, *20*). In these ^{18}O exchange experiments, the total concentration of all species of CO_2 is 25 mM. Hence, in this work $[CO_2] \ll K_{eff}{}^{S}$; similar arguments pertain to bicarbonate binding (*19*).

A second rate determined by the ^{18}O exchange method is R_{H_2O}, the rate of release from the enzyme of water bearing substrate oxygen (eq 4). This is the component of the ^{18}O exchange that is enhanced by exogenous proton donors (*18*). In such enhancements, the exogenous donor acts as a second substrate in the catalysis providing a proton (eq 4), and the resulting effect on ^{18}O exchange is described by eq 6. Here

$$R_{H_2O}/[E] = k_B{}^{obs}[B]/(K_{eff}{}^{B} + [B]) + R_{H_2O}{}^{0}/[E] \quad (6)$$

$k_B{}^{obs}$ is the observed maximal rate constant for the release of $H_2{}^{18}O$ to bulk water caused by the addition of the buffer. $K_{eff}{}^{B}$ is an apparent binding constant of the buffer to the enzyme, [E] and [B] are the concentrations of total enzyme and total buffer, and $R_{H_2O}{}^{0}$ is the rate of release of $H_2{}^{18}O$ into solvent water in the absence of buffer and represents the contribution to proton transfer from other sites on the enzyme or possibly solvent water itself.

With the addition of exogenous proton donors at concentrations up to 200 mM, we have observed a weak inhibition of both R_1 and R_{H_2O}. This is possibly due to the binding of the donors, which are derivatives of imidazole and pyridine, to the zinc in the manner found for the binding of imidazole to carbonic anhydrase I (*21*). The binding constant K_i for this inhibition is generally greater than 100 mM, indicating weak binding at the inhibitory site. Some exogenous donors exhibited no inhibition. In each case of inhibition, a single value K_i described inhibition of both R_1 and R_{H_2O}, as determined by these equations: $R_1^{obs} = R_1/(1 + [B]/K_i)$ and $R_{H_2O}^{obs} = R_{H_2O}/(1 + [B]/K_i)$.

The pH dependence of $R_{H_2O}/[E]$ is often bell shaped, consistent with the transfer of a proton from a single predominant donor to the zinc-bound hydroxide. In these cases the pH profile is adequately fit by eq 7 in which k_B is a pH-independent rate constant for proton transfer and $(K_a)_{donor}$ and $(K_a)_{ZnH_2O}$ are the noninteracting ionization constants of the proton donor BH of eq 4 and the zinc-bound water. The pH dependence of k_B^{obs}/K_{eff}^B depends on the

$$k_B^{obs} = k_B/\{(1 + (K_a)_{donor}/[H^+])(1 + [H^+]/(K_a)_{ZnH_2O})\} \quad (7)$$

ionization state of the zinc-bound water (*2*, *3*).

$$\frac{k_B^{obs}}{K_{eff}^B} = \frac{k_B}{K_{eff}^B}\left(1 + \frac{[H^+]}{(K_a)_{ZnH_2O}}\right)^{-1} \quad (8)$$

Stopped-Flow Spectrophotometry. Initial rates of CO_2 hydration were measured by the changing pH indicator method of Khalifah (*22*) using an Applied Photophysics SX.18MV stopped-flow spectrophotometer. Saturated solutions of CO_2 were prepared by bubbling CO_2 into water at 25 °C. Concentrations of CO_2 (0.5−17 mM) were made by diluting this saturated solution using syringes with gastight seals. Various concentrations of the buffer 4-methylimidazole were used with the indicator phenol red (2.0×10^{-5} M) measured at 557 nm, and imidazole was used with *p*-nitrophenol measured at 400 nm. The total ionic strength of the solution was maintained at a minimum of 0.2 M by addition of the appropriate amount of Na_2SO_4. The mean of four to eight reaction traces of the first 5−10% of the reaction was used to determine initial rates. The uncatalyzed rates were subtracted, and the steady-state constants k_{cat}/K_m and k_{cat} were determined by a nonlinear least-squares method (Enzfitter, Elsevier-Biosoft). Enhancement by exogenous proton acceptors in CO_2 hydration can be described by ping-pong kinetics (*2*−*4*, *6*)

$$\frac{v}{[E]} = \frac{k_{cat}[B]}{K_m^B + [B]\left(1 + \frac{K_m^{CO_2}}{[CO_2]}\right)} \quad (9)$$

from which (extrapolated to saturating CO_2)

$$k_{cat}^{obs} = \frac{k_{cat}[B]}{K_m^B + [B]} \quad (10)$$

Crystallography. Crystals of H64A HCA II were produced by the hanging drop vapor diffusion method and soaked with 4-MI as previously described (*7*). High-resolution X-ray diffraction data (1.05 Å resolution) were collected at the Cornell High Energy Synchrotron Source (CHESS) F1 station using a wavelength of 0.938 Å and a Quantum4 CCD detector system. Additional moderate resolution diffraction data (1.6 Å resolution) were collected using an R-AXIS IV++ image plate system with osmic mirrors and a Rigaku HU-H3R CU rotating anode. The high-resolution data were collected using a 0.2 mm collimator with a crystal to detector distance of 90 mm and an exposure time of 30 s per frame. The moderate resolution data were collected using a 0.3 mm collimator with a crystal to detector distance of 100 mm and an expose time of 600 s per frame. All of the data were collected with the 2θ angle fixed at 0° at a temperature of 100 K using an Oxford Cryostream. The high-resolution data were from 160° collected frames obtained from two crystals, and the medium resolution data were from 330° collected frames from a single crystal. The crystals belong to the space group $P2_1$ with unit cell parameters ($a = 42.1$, $b = 41.5$, $c = 72.1$ Å, and $\beta = 104.3°$). The high-resolution data set was reduced to 92753 reflections (82.4% complete) resulting in an $R_{sym} = 0.126$. The moderate resolution data were reduced to 28456 reflections (88.8% complete) resulting in an R_{sym} of 0.047. X-ray data processing was performed using the DENZO software and scaled with SCALEPACK (*23*).

The overall combined data set (high and moderate resolution data) was scaled to 1.05 Å using SCALEPACK (*23*), giving 93527 independent reflections resulting in $R_{sym} = 0.106$ (31.6 outer resolution shell) and an overall completeness of 83.1% (40.6% outer resolution shell). The R_{sym} is defined as $R_{sym} = \sum(ABS(I - \langle I \rangle))/\sum(I)$, where I is the intensity of an individual reflection and $\langle I \rangle$ is the average intensity for this reflection; the summation is over all intensities.

The structure was refined using the software package CNS (*24*) and SHELX97 (*25*) starting with the previously determined 1.6 Å resolution structure (PDB accession code 1G0X) (*7*) using interactive building with the program O, version 7 (*26*). The final model was refined to 1.05 Å resolution, allowing for full anisotropic least-squares refinement. The refined model has a conventional *R* factor of 16.2% for all reflections. A full account of the experimental details and results of the refinement of the model will be published elsewhere.

Structural Alignment. The least-squares structural superimposition between the H64A HCA II and the rat form of CA III (PDB accession code 1FLJ) (*11*) was performed using the least-squares algorithm contained in the molecular modeling program O, version 7 (*26*). The root-mean-square deviation between the structures is 0.81 Å.

RESULTS

Kinetics. The rate constant $R_{H_2O}/[E]$ measures the proton transfer dependent release of ^{18}O-labeled water from the enzyme (eq 4). The activation of $R_{H_2O}/[E]$ by the exogenous proton donor 4-MI, measured in the dehydration direction by ^{18}O exchange, was observed to be a saturable process for H64A and W5A-H64A HCA II; moreover, the extent of activation was equivalent for both mutants (Figure 1). The enhancement of this catalysis by wild-type HCA II and H64A HCA II by 4-MI was previously reported (see Figure 5 of

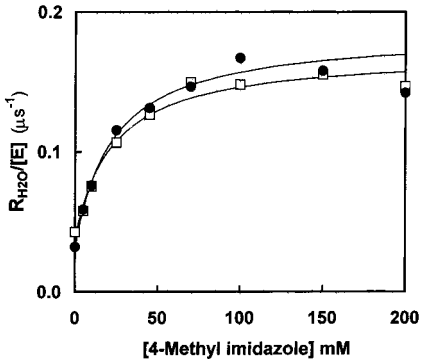

FIGURE 1: Dependence of R_{H_2O}/[E] (μs^{-1}) on the concentration of the exogenous proton donor 4-methylimidazole (4-MI) for catalysis by (●) H64A HCA II and (□) W5A-H64A HCA II. Data were obtained by ^{18}O exchange. The pH was 7.8, the ionic strength was maintained at a minimum of 0.2 M by addition of Na_2SO_4, and the temperature was 25 °C. The solid lines are a fit of eq 6 to the data with parameters given in Table 1. A weak inhibition at larger concentrations of 4-MI was neglected in the fit.

Table 1: Enhancement by the Exogenous Proton Donor 4-Methylimidazole of Catalysis of ^{18}O Exchange by Variants of Human Carbonic Anhydrase II at pH 7.8 and 25 °C[a]

enzyme	k_B^{obs} (μs^{-1})	K_{eff}^B (mM)
wild type[b]	0.10 ± 0.01	4 ± 2
H64A[b]	0.12 ± 0.01	25 ± 4
W5A-H64A	0.11 ± 0.01	17 ± 8
W5L-H64A	0.14 ± 0.01	16 ± 3
W5F-H64A	0.16 ± 0.02	38 ± 11

[a] These data were obtained by a fit of the constants k_B^{obs} and K_{eff}^B of eq 6 to data for the enhancement of R_{H_2O}/[E] using the conditions listed in Figure 1. In each case there was a weak inhibition of ^{18}O exchange at higher concentrations of 4-methylimidazole characterized by an inhibition constant K_i of approximately 130−150 mM that was evident in both R_{H_2O} (Figure 1) and R_1 (data not shown). This inhibition was neglected in determining the values of this table. [b] Data from Duda et al. (*7*).

ref *7*). These data were adequately fit to eq 6 describing 4-MI as a second substrate of the catalysis with the constants of eq 6 given in Table 1. The additional mutants W5L-H64A and W5F-H64A HCA II were also activated by 4-MI in a manner similar to the activation of H64A HCA II (Table 1). Comparison of the values of R_1 for the hydration of CO_2-catalyzed H64A and W5A-H64A HCA II showed no appreciable differences as 4-MI was added up to 200 mM (data for R_1 for H64A HCA II are presented in ref *7*). It was more apparent from R_1 than R_{H_2O} that addition of 4-MI caused a weak inhibition of these enzymes (data shown for H64A in ref *7*). This is possibly due to the binding of 4-MI to the zinc, similar perhaps to the binding of imidazole to HCA I (*21*), although no such observation was made in the 1.05 Å resolution structure reported in this paper. The value of the inhibition constant was too large to measure accurately in this work but is estimated roughly at >100 mM for each of the variants of HCA II listed in Table 1. Since our substrate concentrations were much less than K_{eff}^S of eq 5, we could not differentiate between competitive and noncompetitive modes of inhibition.

4-MI acting as a proton acceptor was also an activator of k_{cat} for the hydration of CO_2 catalyzed by H64A and W5A-H64A HCA II and measured by stopped-flow spectrophotometry. Again, the extent of activation was saturable for both mutants, with the double mutant activated to an extent

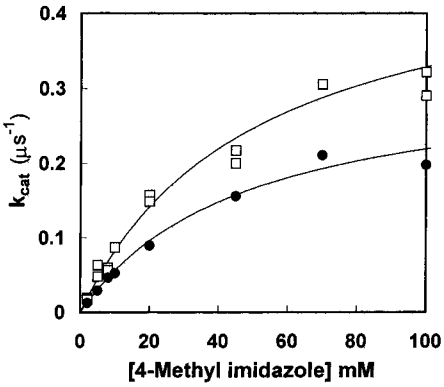

FIGURE 2: Dependence of k_{cat}^{obs} (μs^{-1}) for hydration of CO_2 on the concentration of the exogenous proton donor 4-methylimidazole for catalysis by (●) H64A HCA II and (□) W5A-H64A HCA II. Data were determined by stopped-flow spectrophotometry. The pH was 7.8, the ionic strength was maintained at a minimum of 0.2 M by addition of Na_2SO_4, and the temperature was 25 °C. For H64A HCA II the maximal value of $k_{cat} = 0.32 \pm 0.04$ μs^{-1} and $K_m^B = 47 \pm 12$ mM; for W5A-H64A HCA II the maximal value of $k_{cat} = 0.45 \pm 0.04$ μs^{-1} and $K_m^B = 41 \pm 10$ mM (in eq 10).

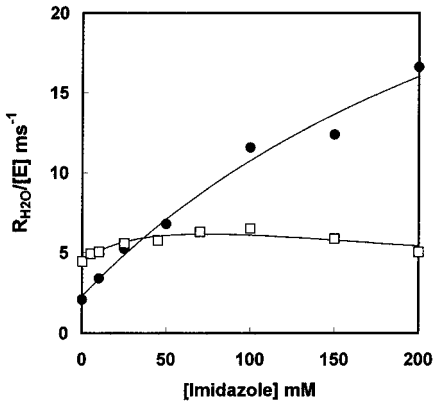

FIGURE 3: Dependence of R_{H_2O}/[E] (ms^{-1}) on the concentration of the exogenous proton donor imidazole for catalysis by (●) wild-type HCA III and (□) W5A HCA III. The pH was 7.3, the ionic strength was maintained at a minimum of 0.2 M by addition of Na_2SO_4, and the temperature was 25 °C.

about 50% greater than the H64A (Figure 2;, values of the parameters of eq 10 are given in the legend to Figure 2).

We observed significant differences in activation by the exogenous proton donor imidazole of wild-type HCA III and W5A HCA III. Figure 3 shows the substantial activation of R_{H_2O}/[E] for wild-type HCA III that appears to be approaching saturation at very large concentrations of imidazole. In contrast, there was no significant enhancement of catalysis by W5A HCA III upon increasing concentrations of imidazole (Figure 3). A similar response was seen in stopped-flow measurements of k_{cat} for the hydration of CO_2; wild-type HCA III showed activation by imidazole that was much greater than the response of W5A HCA III (Figure 4). Again, addition of imidazole to HCA III has been shown not to affect k_{cat}/K_m and R_1 (*27*). We measured the effect of 4-MI on ^{18}O exchange catalyzed by wild-type and W5A HCA III. For wild-type HCA III, 4-MI caused a 2-fold increase in R_{H_2O}/[E] at saturation. However, there was an inhibitory effect of 4-MI on W5A HCAIII that made interpretation of catalysis difficult.

We compared the enhancement by 4-MI of ^{18}O exchange catalyzed by H64A HCA II with the enhancement by a

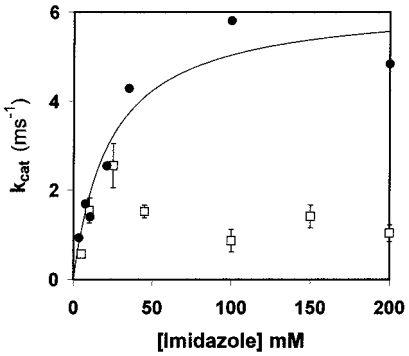

FIGURE 4: Dependence of k_{cat}^{obs} (ms^{-1}) for hydration of CO_2 on the concentration of the exogenous proton donor imidazole for catalysis by (●) wild-type HCA III and (□) W5A HCA III. The pH was 6.8, the ionic strength was maintained at a minimum of 0.2 M by addition of Na_2SO_4, and the temperature was 25 °C. The data for wild-type HCA III are from Tu et al. (*27*).

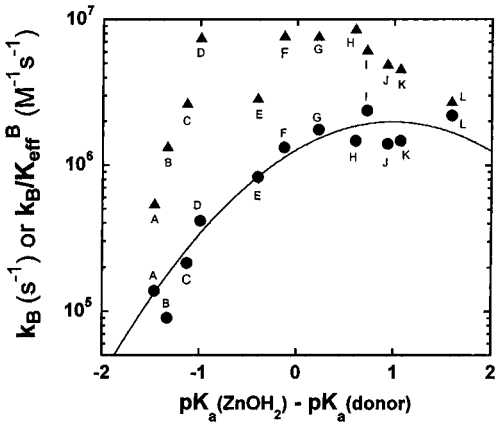

FIGURE 5: Values of (●) the rate constant for proton transfer k_B (s^{-1}) and (▲) the rate constant k_B/K_{eff}^B (M^{-1} s^{-1}) for catalysis by H64A HCA II plotted versus the difference in pK_a values of the zinc-bound water and the exogenous proton donor. Conditions were as described in Figure 1, except the pH of each experiment was at the pK_a of the exogenous donor used. The following are the individual proton donors with their corresponding solution values of pK_a under our conditions: A, 1,2-dimethylimidazole (8.3); B, 2-methylimidazole (8.2); C, 2-ethylimidazole (8.0); D, 4-methylimidazole (7.9); E, 1-methylimidazole (7.3); F, imidazole (7.0); G, 3,4-dimethylpyridine (6.6); H, 3,5-dimethylpyridine (6.3); I, 4-methylpyridine (6.1); J, 1-vinylimidazole (5.9); K, 3-methylpyridine (5.8); L, pyridine (5.3). The standard errors of individual points are 15% or less. The solid line is a fit of the Marcus equation[2] to the data for k_B with parameters given in Table 2.

number of imidazole and pyridine derivatives. Estimates of the rate constant k_B for proton transfer from these exogenous proton donors to the zinc-bound hydroxide (eq 4) are shown in Figure 5 and were made by two procedures. First, in several cases a full bell-shaped pH profile was obtained, using a concentration of exogenous donor that saturated the activation, indicating predominant proton transfer between the exogenous donor and zinc-bound hydroxide (*18*). This was demonstrated for activation by 4-MI (Figure 6 and Table 4 of ref *7*). We were able to estimate the pH-independent rate constant k_B and values of the pK_a of the donor and acceptor by a least-squares fit of eq 7 to the data. We found that the pK_a for the donor obtained in this manner agreed within 0.3 pK_a unit with the solution pK_a of the exogenous donor. The pK_a of the zinc-bound water was determined to be near 7.1 for the forms of HCA II used here, consistent with the data of Duda et al. (*7*). Second, for each proton

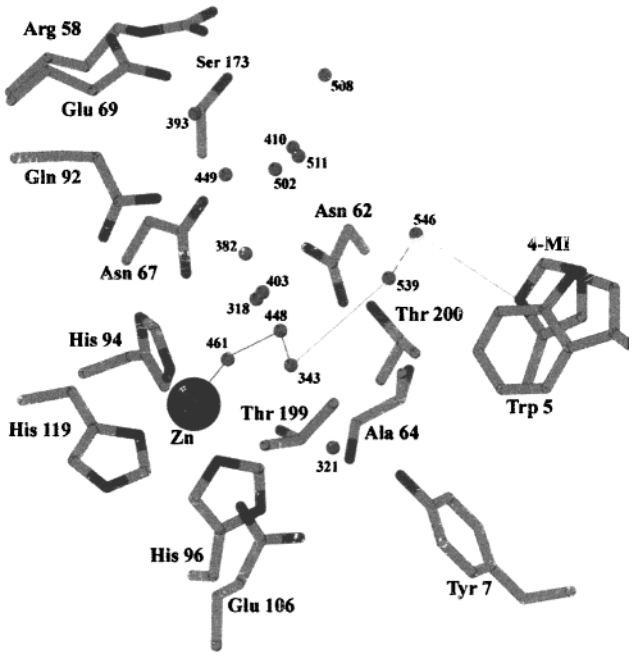

FIGURE 6: Stick diagram depicting the location of the binding site of 4-methylimidazole (4-MI) and water molecules in the active site cavity of H64A HCA II. The zinc (large sphere) is coordinated by His 94, 96, and 119; 4-MI is shown in a π-stacking interaction with the indole ring of Trp 5. Also included are the positions of the oxygen atoms of various water molecules found in the active site cavity (small spheres). Water 461 is the zinc-bound water. There is no direct hydrogen-bonded water chain connecting water 461 with 4-MI, although a weak electrostatic network of four water molecules (448, 343, 539, 546) can be traced. The lines drawn joining these waters represent hydrogen-bonding (black) and weak electrostatic (gray) interactions.

donor an estimate of the maximum value of R_{H_2O}/[E] was made by fitting eq 6 to the activation curve, such as shown for 4-MI in Figure 1. Then by estimating the pK_a of the bound donors with their solution values, we applied eq 7 to obtain k_B. The values of k_B determined by these two procedures were in reasonable agreement, especially for the purposes of making a free energy plot which covers over 2 orders of magnitude, shown in Figure 5. Values of the pH-independent rate constant k_B/K_{eff}^B, shown in Figure 5, were determined by a fit of eqs 6 and 8.

Crystallography. We have extended to 1.05 Å our earlier studies at 1.6 Å (*7*) of the complex showing 4-MI bound to H64A HCA II. This has allowed us to determine with more precision the locations of ordered water molecules in the active site cavity, which have not been previously reported for this complex. We are particularly interested in possible proton transfer pathways between the proton acceptors/donors and the zinc-bound hydroxide/water. As reported by Duda et al. (*7*), 4-MI is bound in a π-stacking interaction with the indole ring of Trp 5 in H64A HCA II. There are no other interactions of 4-MI with side chains or the backbone of the enzyme, allowing the N1 and N3 nitrogens to be accessible to the solvent in the active site cavity. Thus 4-MI extends into the active site cavity at a location that overlaps that of the side chain of His 64 in the out position of HCA II. The electron density map of the 4-MI complex with H64A HCA II has identified 16 water molecules, in addition to the zinc-bound water, in the active site cavity; these have temperature or *B* factors between 25 and 30 $Å^2$, comparable to the *B* factors of various side chains that extend into the active site

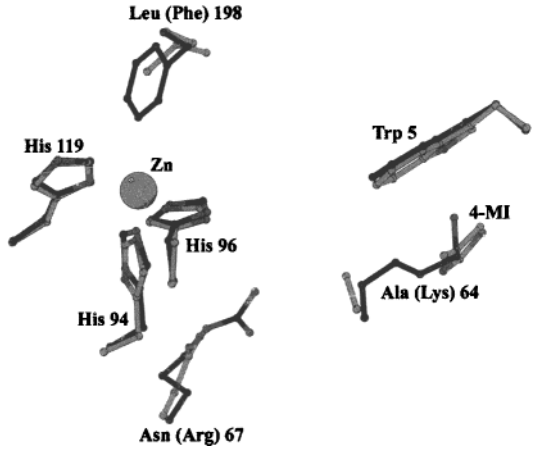

FIGURE 7: Structural overlay of the active site region of H64A CA II (black) and rat CA III (gray) from Mallis et al. (*11*). Residues Trp 5 and His 94, 96, and 119 are conserved between the two isozymes, whereas Asn 67, Ala 64, and Leu 198 in H64A HCA II are Arg, Lys, and Phe, respectively, in rat CA III (given in parentheses).

(Figure 6). The distance between the zinc-bound water and the N1 of 4-MI is 11.6 Å. The crystal structure shows no obvious hydrogen-bonded pathway for proton transfer between the zinc-bound water and the position of 4-MI. The distance of the nearest water molecule (water 546) to 4-MI (Figure 6) is 4.0 Å, too far for a hydrogen bond. The only traceable water chain linking the zinc-bound water (water 461) and N1 of 4-MI is through a weak electrostatic network of four water molecules (448, 343, 539, and 546). Two of these links (between water 343 and 539 at 3.9 Å and between water 546 and the N1 of 4-MI at 4.0 Å) are too distant to be considered hydrogen bonds although weak electrostatic communication could be feasible.

DISCUSSION

This study combines the kinetics of chemical rescue and crystallography to comment on the location of proton transfer sites in carbonic anhydrase. The data of Figures 1 and 2 indicate that the binding site of 4-MI at Trp 5 observed in the crystal structure of H64A HCA II (Figure 6) is a nonproductive binding site. It is possible although less likely that Trp 5 is a productive binding site and in its absence in W5A-H64A HCA II there exist similarly effective pathways for proton transfer between 4-MI and the zinc-bound solvent. In contrast to isozyme II, the replacement of Trp 5 by Ala in HCA III abolished chemical rescue of k_{cat} and R_{H_2O} by imidazole but left k_{cat}/K_m for hydration unchanged (Figures 3 and 4). These data suggest that in HCA III the binding of imidazole to Trp 5 is a productive binding site. A less likely interpretation is that Trp 5 is not a productive binding site in HCA III and that the replacement of Trp 5 caused structural changes that abolished chemical rescue at another binding site.

CA III has a backbone structure which is very closely superimposable with CA II, especially in the region of the active site (*11*, *28*). Moreover, HCA II and III contain Trp 5 in the same location and orientation in the cavity (Figure 7). For HCA III, the extent of activation of the rate constant for ^{18}O release from the enzyme $R_{H_2O}/[E]$ at 200 mM imidazole was about 10^4 s^{-1} (Figure 3). If this magnitude of activation occurred with 4-MI bound to Trp 5 in H64A HCA II, it would barely make a significant contribution to the plateau observed near 10^5 s^{-1} of Figure 1. Hence, our overall results may indicate that imidazole donors bind to Trp 5 on both H64A HCA II and HCA III and transfer protons in catalysis but that there are other more productive binding sites for H64A HCA II.

Hence, the data indicate that 4-MI bound to Trp 5 is a nonproductive binding site in H64A HCA II; that is, it does not significantly contribute to chemical rescue. This study emphasizes a caution already made in connection with nonproductive binding sites in chemical rescue of nucleoside diphosphate kinase (*29*), that interpretation of maximal velocities of chemical rescue in catalysis is possibly affected by nonproductive binding (*30*). Moreover, knowledge that the observed binding site of 4-MI (Figure 6) is nonproductive in proton transfer provides a useful insight into catalysis by wild-type HCA II. Duda et al. (*7*) showed the overlap of the binding site of 4-MI in H64A HCA II and the out position of His 64 in wild-type HCA II. Because of this overlap we can comment that the out position of His 64 considered alone is unlikely to be involved in proton transfer. That is, either the "in" position is active in proton transfer or the side chain of His 64 must have the flexibility of occupying both the in and out positions in order to effectively shuttle protons between the zinc-bound solvent molecule and bulk solvent.

The nonproductive binding site of 4-MI at Trp 5 has the N1 and N3 positions of 4-MI at 13.4 and 12.1 Å from the zinc (Figure 6). This suggests that this site may be too distant for effective proton transfer at rates in excess of 10^5 s^{-1} achieved by carbonic anhydrase II. The crystal structure at 1.05 Å does not show a plausible hydrogen-bonded water chain connecting the zinc-bound water and 4-MI (Figure 6). This is not evidence against a viable proton transfer pathway, of course, which may not be observable in a crystal structure. Efficient proton transfer in wild-type HCA II involves His 64, which in the in position is about 7.5 Å from the zinc. At this distance, two water molecules can form a hydrogen-bonded bridge between the imidazole ring of His 64 and the zinc-bound water. It would require three or four water molecules to span the gap between the zinc-bound water and 4-MI in Figure 6. These observations appear to agree with those made by Jude et al. (*31*), who determined the crystal structure of a mutant of CA V chemically modified with 4-(chloromethyl)imidazole to contain a proton shuttle residue in the active site cavity. Jude et al. suggested that a functional proton shuttle requires conformational flexibility to transport protons rapidly between the active site and solvent, and the shuttle must be located close enough to be connected to the zinc-bound solvent by no more than two or three water molecules.

The data of Figures 3 and 4 indicate that Trp 5 in HCA III is a predominant and productive binding site. There may be fewer possible productive sites in HCA III, and fewer possible proton transfer pathways, than in HCA II because of the different environment of the active site cavities of HCA II and HCA III; there are more steric constraints and positively charged residues in HCA III (Figure 7). There is not a crystal structure of HCA III available; there are, however, structures available for bovine (*28*) and rat (*11*) CA III. These structures can be examined for clues as to the difference in the role of proton transfer. First, isozyme III is much less efficient in proton transfer than isozyme II. Even

Table 2: Constants of the Marcus Theory for Inter- and Intramolecular Proton Transfer in Catalysis by Variants of Carbonic Anhydrase[a]

system	proton donor	$\Delta G^{\ddagger}_0$ (kcal/mol)	w^r (kcal/mol)	w^p (kcal/mol)
intermolecular				
CA II[b]	buffers	0.5 ± 0.1	8.8 ± 0.1	8.5 ± 0.2
CA V[c]	buffers	0.8 ± 0.5	10.0 ± 0.2	8.2 ± 1.0
intramolecular				
CA III	His 64[d]	1.4 ± 0.3	10.0 ± 0.2	5.9 ± 1.1
	His 67[e]	1.3 ± 0.3	10.9 ± 0.1	5.9 ± 1.1
	Glu or Asp 64[f]	2.2 ± 0.5	10.8 ± 0.1	4.0 ± 1.6
nonenzymic	buffer to buffer[g]	2.0	3.0	

[a] The data were obtained by a least-squares fit of the Marcus equation[2] to rate constants for proton transfer k_B such as shown in Figure 5. $\Delta G^{\ddagger}_0$ is the intrinsic kinetic barrier and $w^r$and w^p are the work functions or thermodynamic terms for the dehydration and hydration directions, respectively. [b] This work. Here the variant is H64A HCA II. [c] From Earnhardt et al. (*33*); the variant is a truncation mutant of murine CA V in which the C-terminal residue is Ser 22 in the conventional carbonic anhydrase numbering scheme. [d] Reference *17*. [e] Reference *36*. [f] Reference *37*. [g] Reference *35*.

with the mutant K64H HCA III which places His 64 in the active site, the rate constant for proton transfer is 10−100-fold less than in HCA II (*32*). However, the backbone conformations of rat CA III and HCA II are very closely superimposable with a root-mean-square deviation of 0.81 Å for backbone atoms. Prominent side chains in the active site cavity of CA II and III are shown in Figure 7. The cavity for CA III is much more sterically constrained and contains two positively charged residues (Lys 64 and Arg 67) not present in HCA II. Thus the array of binding sites for imidazole may be different in HCA III compared with available sites in H64A HCA II, although both may involve Trp 5 in some manner. In addition, the more constrained and more electrostatically charged cavity in CA III may increase the energy barrier for construction of a hydrogen-bonded water chain connecting the zinc-bound water and the imidazole binding site.

An additional feature of proton transfer in catalysis by H64A HCA II is the continuous free energy plot for the rate constant for proton transfer k_B with derivatives of imidazole and pyridine ions as proton donors (Figure 5). Using a similar set of imidazole and pyridine derivatives, Earnhardt et al. (*33*) carried out the same experiment as in Figure 5 using a truncated form of CA V in which 20 residues from the amino-terminal end were deleted. Their example does not have a residue 5, and yet their results are very similar to those of this study (compared in Table 2), emphasizing our conclusion that the predominant binding site of these exogenous buffers is not Trp 5. The solid line of Figure 5 is the fit of the Marcus rate theory to k_B. Table 2 gives the resulting values of the intrinsic kinetic barrier $\Delta G^{\ddagger}_0$ and the work function or thermodynamic contribution w^r (dehydration direction) to the proton transfer (*17*, *34*, *35*).[2] These data demonstrate a general result that has also been observed for intramolecular proton transfer in HCA III (*17*, *36*, *37*) and for intermolecular proton transfer involving exogenous donors in CA V (*33*); in this application of Marcus theory to proton transfer in carbonic anhydrase the intrinsic barrier $\Delta G^{\ddagger}_0$ is small, less than 2 kcal/mol, and the work functions are large, generally 6−11 kcal/mol (Table 2). The data for H64A HCA II obtained here are qualitatively similar to those of the previous studies in Table 2. These parameters of the application of Marcus theory have been interpreted to signify a very rapid and facile proton transfer preceded by an unfavorable preequilibrium in which the active site cavity including water molecules attains conformations that allow a rapid proton transfer (*17*).

However, in view of the existence of nonproductive binding sites, we must consider that values of k_B obtained for exogenous proton donors are affected. We observed the unusually low values of $\Delta G^{\ddagger}_0$ of less than 1 kcal/mol for the two examples of intermolecular proton transfer; these data may be affected by the presence of nonproductive binding sites. We point out that considerations of nonproductive binding are less of a concern in the free energy plots of k_B for mutants of K64H (*17*), R67H (*36*), and K64E HCA III (*37*), since these are cases of intramolecular proton transfer (although we may still need to account for conformational states of these side chains that are not involved in proton transfer). Accordingly, the values of $\Delta G^{\ddagger}_0$ for the intramolecular proton transfer are larger and similar to the values anticipated from the nonenzymic bimolecular case (Table 2). Another feature for consideration in Figure 5 is that the entries for the pyridine derivatives occur separated from the entries for the imidazole derivatives (with the exception of 1-vinylimidazole) because the values of the pK_a for the pyridine-type proton donors are smaller. In fact, 1-vinylimidazole does have a pK_a (5.9) in the region of those of the pyridine derivatives (see legend to Figure 5), and the value of k_B due to proton transfer from 1-vinylimidazolium appears consistent in Figure 5 with the pyridine entries. However, a different array of productive and nonproductive binding sites for pyridine compared with imidazole derivatives could influence Figure 5. In fact, Duda et al. (personal communication) have found that crystals of H64A HCA II diffused with pyridine show that this exogenous proton donor binds in a π-stacking complex with Phe 131 in the active site cavity and not with Trp 5.

We therefore consider the second-order rate constants describing the proton transfer k_B/K_{eff}^B determined using eqs 6 and 8 from the ^{18}O exchange studies for proton transfer in the dehydration direction. These rate constants are not affected by nonproductive binding (*30*) but show considerably more scatter than the values of k_B (Figure 5). The scatter

[2] The observed overall activation energy for proton transfer $\Delta G^{\ddagger}$ is described in Marcus theory in terms of two variables, the standard free energy of reaction ΔG° and an intrinsic kinetic barrier $\Delta G^{\ddagger}_0$, which is the value of $\Delta G^{\ddagger}$ when $\Delta G^{\circ} = 0$, that is, when the transfer is free of thermodynamic influences and represents a pure or "intrinsic" energy barrier. The Marcus equation is further modified to describe proton transfers in which there is a component of the observed activation barrier that does not depend on ΔG° for the reaction. This component is called the work term w^r. In nonenzymic, bimolecular proton transfers, the work term is considered part of the free energy of reaction needed to bring the reactants together, form the reaction complex, and reorganize the solvent structure prior to proton transfer. Similarly, w^p is the work term required for the reverse reaction: $\Delta G^{\ddagger}_{obs} = w^r + [1 + (\Delta G^{\circ}_{obs} - w^r + w^p)/4\Delta G^{\ddagger}_0]^2 \Delta G^{\ddagger}_0$. Use of this expression assumes that the work terms w^r and w^p as well as the intrinsic energy barrier $\Delta G^{\ddagger}_0$ do not vary for proton transfer between the series of homologous proton donors and acceptors to which the equation is fit. In this work, the observed activation barrier is obtained from k_B, the experimental rate constant for proton transfer, $\Delta G^{\ddagger}_{obs} = -RT \ln(hk_B/kT)$, where h is the Planck constant and k is the Boltzmann constant; and the observed free energy of reaction is obtained from ΔpK_a of the reactants, $\Delta G^{\circ}_{obs} = RT \ln[(K_a)_{acceptor}/(K_a)_{donor}]$.

suggests different binding sites or orientations in binding sites for different exogenous donors with varied contributions to proton transfer as measured by k_B/K_{eff}^B. With values near 10^7 M^{-1} s^{-1}, k_B/K_{eff}^B is clearly not diffusion-controlled. In this aspect the data are different from analogous experiments with wild-type HCA II for which k_{cat}/K_m at 10^9 M^{-1} s^{-1} does approach diffusion control (*38*). Wild-type HCA II has His 64 as a proton shuttle accessible near the surface of the enzyme and is efficient in proton transfer. H64A HCA II would require the exogenous proton donor to move deeply into the active site cavity. The scatter of points for k_B/K_{eff}^B for buffer activation of H64A HCA II in Figure 5 is greater than the scatter in equivalent measurements for wild-type HCA II (*38*). This most likely reflects specific interactions between the exogenous donors and their binding sites in the active site cavity and causes scatter in the free energy plot of Figure 5.

ACKNOWLEDGMENT

We thank the staff at the Cornell High Energy Synchrotron Source (CHESS) for help and support at the F1 station during X-ray data collection. We also acknowledge the excellent technical assistance of Ke Ren.

REFERENCES

1. Hewett-Emmett, D., and Tashian, R. E. (1996) *Mol. Phylogenet. Evol. 5*, 50−77.
2. Lindskog, S. (1997) *Pharmacol. Ther. 74*, 1−20.
3. Christianson, D. W., and Fierke, C. A. (1996) *Acc. Chem. Res. 29*, 331−339.
4. Steiner, H., Jonsson, B.-H., and Lindskog, S. (1975) *Eur. J. Biochem. 59*, 253−259.
5. Tu, C. K., Silverman, D. N., Forsman, C., Jonsson, B. H., and Lindskog, S. (1989) *Biochemistry 28*, 7913−7918.
6. Silverman, D. N., and Lindskog, S. (1988) *Acc. Chem. Res. 21*, 30−36.
7. Duda, D., Tu, C. K., Qian, M., Laipis, P. J., Agbandje-McKenna, M., Silverman, D. N., and McKenna, R. (2001) *Biochemistry 40*, 1741−1748.
8. Nair, S. K., and Christianson, D. W. (1991) *J. Am. Chem. Soc. 113*, 9455−9458.
9. Briganti, F., Mangani, S., Orioli, P., Scozzafava, A., Vernaglione, G., and Supuran, C. T. (1997) *Biochemistry 36*, 10384−10392.
10. Eriksson, A. E., Jones, T. A., and Liljas, A. (1988) *Proteins: Struct., Funct., Genet. 4*, 274−282.
11. Mallis, R. J., Paland, B. W., Chatterjee, T. K., Fisher R. A., Darmawan, S., Honzatko, R. B., and Thomas, J. A. (2000) *FEBS Lett. 482*, 237−241.
12. Tanhauser, S. M., Jewell, D. A., Tu, C. K., Silverman, D. N., and Laipis, P. J. (1992) *Gene 117*, 113−117.
13. Studier, F. W., Rosenberg, A. H., Dunn, J. J., and Dubendorf, J. W. (1990) *Methods Enzymol. 185*, 60−89.
14. Khalifah, R. G., Strader, D. J., Bryant, S. H., and Gibson, S. M. (1977) *Biochemistry 16*, 2241−2247.
15. Tu, C. K., Thomas, H. G., Wynns, G. C., and Silverman, D. N. (1986) *J. Biol. Chem. 261*, 10100−10103.
16. Engberg, P., Millqvist, E., Pohl, G., and Lindskog, S. (1985) *Arch. Biochem. Biophys. 241*, 628−638.
17. Silverman, D. N., Tu, C. K., Chen, X., Tanhauser, S. M., Kresge, A. J., and Laipis, P. J. (1993) *Biochemistry 32*, 10757−10762.
18. Silverman, D. N. (1982) *Methods Enzymol. 87*, 732−752.
19. Simonsson, I., Jonsson, B.-H., and Lindskog, S. (1979) *Eur. J. Biochem. 93*, 409−417.
20. Krebs, J. F., Rana, R., Dluhy, R. A., and Fierke, C. A. (1993) *Biochemistry 32*, 4496−4505.
21. Kannan, K. K., Petef, M., Fridborg, K., Cid-Dresdner, H., and Lovgren, S. (1977) *FEBS Lett. 73*, 115−119.
22. Khalifah, R. G. (1971) *J. Biol. Chem. 246*, 2561−2573.
23. Otwinowski, Z., and Minor, W. (1997) *Methods Enzymol. 276*, 307−326.
24. Brünger, A. T., Adams, P. D., Clore, G. M., DeLano, W. L., Gross, P., Grosse-Kunstleve, R. W., Jiang, J. S., Kuszewski, J., Nilges, M., Pannu, N. S., Read, R. J., Rice, L. M., Simonson, T., and Warren, G. L. (1998) *Acta Crystallogr. D54*, 905−921.
25. Sheldrick, G. M., and Shneider, T. R. (1997) *Methods Enzymol. 277*, 319−343.
26. Jones, T. A., Zou, J. Y., Cowan, S. W., and Kjeldgaard, M. (1991) *Acta Crystallogr., Sect. A 47*, 110−119.
27. Tu, C. K., Paranawithana, S. R., Jewell, D. A., Tanhauser, S. M., LoGrasso, P. V., Wynns, G. C., Laipis, P. J., and Silverman, D. N. (1990) *Biochemistry 29*, 6400−6405.
28. Eriksson, A. E., and Liljas, A. (1993) *Proteins: Struct., Funct., Genet. 16*, 29−42.
29. Admiraal, S. J., Meyer, P., Schneider, B., Deville-Bonne, D., Janin, J., and Herschlag, D. (2001) *Biochemistry 40*, 403−413.
30. Fersht, A. (1999) in *Structure and Mechanism in Protein Science*, pp 114−116, W. H. Freeman and Co., New York.
31. Jude, K. M., Wright, K., Tu, C. K., Silverman, D. N., Viola, R. E., and Christianson, D. W. (2001) (submitted for publication).
32. Jewell, D. A., Tu, C. K., Paranawithana, S. R., Tanhauser, S. M., LoGrasso, P. V., Laipis, P. J., and Silverman, D. N. (1991) *Biochemistry 30*, 1484−1490.
33. Earnhardt, J. N., Tu, C. K., and Silverman, D. N. (1999) *Can. J. Chem. 77*, 726−732.
34. Marcus, R. A. (1968) *J. Phys. Chem. 72*, 891−899.
35. Kresge, A. J. (1975) *Acc. Chem. Res. 8*, 354−360.
36. Ren, X., Tu, C. K., Laipis, P. J., and Silverman, D. N. (1995) *Biochemistry 34*, 8492−8498.
37. Qian, M., Tu, C. K., Earnhardt, J. N., Laipis, P. J., and Silverman, D. N. (1997) *Biochemistry 36*, 15758−15764.
38. Rowlett, R. S., and Silverman, D. N. (1982) *J. Am. Chem. Soc. 101*, 6734−6741.

BI0120695